Experimental facility for nanosecond time-resolved, low angle x-ray diffraction experiments using a laser-produced plasma source

J. M. Forsyth and R. D. Frankel

Laboratory for Laser Energetics, University of Rochester, 250 East River Road, Rochester, New York 14623

(Received 8 February 1984; accepted for publication 26 March 1984)

A low angle x-ray diffraction camera that is coupled to a nanosecond laser-produced plasma x-ray source is described. The system includes a grazing incidence toroidal x-ray collector, a digital, intensified, television based x-ray detector, and environmentally controlled sample chamber. The camera is designed for use in time-resolved x-ray diffraction studies. Preliminary kinetics x-ray scattering results from the purple membrane of the *Halobacterium halobium* are presented.

INTRODUCTION

The past few years have seen widespread activity in the development and application of very intense x-ray sources, particularly synchronous electron storage rings.[1,2] An important motivation for this development is the desire to study dynamic processes on the atomic and molecular scale in ordered, or quasiordered systems.[3] With a high-intensity source, data-acquisition times in various x-ray scattering measurements can be reduced to time scales of interest in kinetic experiments. In this paper we report the development of a high-intensity, laser driven, pulsed x-ray source, describe a focusing x-ray diffraction camera constructed to take advantage of the optical properties of the x-ray source, and report briefly on the successful application of this system to structural kinetic studies in photobiology.[4,5] The facility described here can be adapted to perform structural kinetic studies in a wide range of systems including crystallized proteins, membranes, polymers, and solutions, as well as phase transformation and shock induced phenomena in solid-state physics.

The desire to perform time-resolved x-ray scattering measurements places severe performance requirements on the x-ray source parameters such as energy, pulsewidth, wavelength, bandwith, divergence, and degree of synchronization to specimen activity. The specimen to be studied imposes its own constraints on the system such as its degree of atomic order, the reversibility of the kinetic activity, the time scale of its activity, and its susceptibility to x-ray damage. Coupled to these considerations are limitations imposed by detector performance in the areas of time response, linearity, dynamic range, and area of coverage. The system to be described was developed around the specific requirements of x-ray diffraction from biological specimens. The relatively low x-ray scattering efficiency of biological materials and the structural complexity of such systems combined to impose especially severe performance requirements on all system components.

I. SOURCE DESCRIPTION

It is well known that extremely hot plasmas of small dimensions may be formed by focusing high-intensity laser pulses onto solid targets. For laser pulses up to roughly 1-ns duration the hot plasma is unable to flow significantly away from the laser focal volume during the laser pulse. The vigorous heating produced by the laser leads to rapid expansion and cooling of the plasma at the termination of the pulse. Thus, the spatial and temporal characteristics of the laser pulse are reproduced by many components of the hot plasma radiation spectrum. Using multistage Nd^{+3}:glass lasers, constructed in connection with experiments in inertial confinement fusion, plasma electron temperatures of approximately 1 kV may be attained. Under appropriate conditions efficient x-ray production to 5 keV or more may be attained.[6]

The laser used in all of our work to date is the University of Rochester's Glass Development Laser (GDL), a seven-stage, single beam Nd^{+3}:glass laser[7] constructed as a prototype for the 24-beam OMEGA laser system.[8] This laser produces single pulses of selectable duration from 50 ps to 1 ns at a repetition rate of two shots per hour. Single pulse energies of up to 150 J at 1.054 μm are produced in 1-ns pulses. Lower energies but higher powers (25 J at 50 ps) are available in shorter pulses. Total x-ray emission is closely correlated with incident laser energy, thus we generally perform experiments using 1-ns pulses.

The x-ray emission spectrum depends on the choice of target material. Under conditions where the plasma electron temperature is approximately 1 kV, target atoms with atomic numbers roughly in the range from 12 to 25 will be ionized to helium-like or hydrogen-like configurations on a subnanosecond time scale. These ions, collisionally excited in the hot plasma, emit a series of well-separated lines of relatively high oscillator strength. A few of these lines can be foil filtered for applications requiring good spectral purity. Efficient production of such filtered line radiation is presently possible at several discrete wavelengths from 1.5 to 5 Å.[6]

Recent advances in nonlinear optics have made possible the conversion of the infrared output from high peak power Nd^{3+}:glass lasers to the ultraviolet (third harmonic) with intrinsic efficiencies approaching 80%.[9] For the past 2 years such a frequency conversion system has been employed on the GDL facility.[10] There are many benefits to the use of short-wavelength laser radiation in target interaction experiments. Among these are a greatly enhanced degree of collisional absorption of the laser light in the target, and coupling

 0034-6748/84/081235-08$01.30

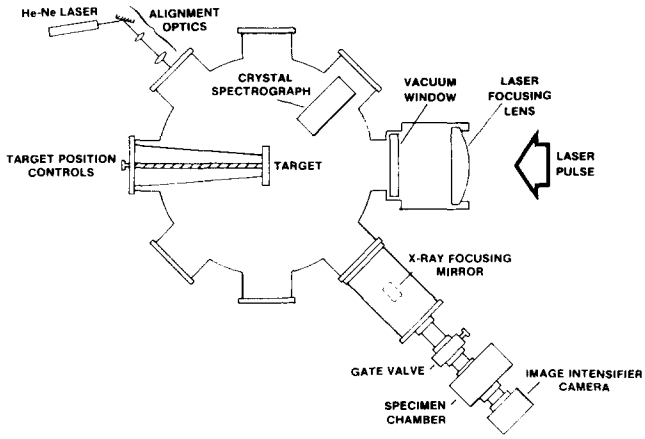

FIG. 1. Schematic of experimental chamber (top view).

of the laser energy into higher density regions of the plasma.[11,12] In our application we observe a tenfold increase in x-ray line emission in the spectral range of 2–5 Å with the use of ultraviolet laser pulses compared to infrared pulses of similar energy.[6] In our biostructural kinetic experiments, all experiments have been performed using the frequency tripled GDL facility.

The output pulses from this laser are focused by an $f/12$, single element, fused silica lens onto targets located in a 24-in.-diam stainless-steel vacuum chamber shown schematically in Fig. 1. Foil targets are placed near the center of the chamber and are mounted on a three-axis positioning system. Alignment of the target with respect to the focal position of the laser pulse is facilitated by the use of a cw argon ion laser (Spectra Physics Model 165) beam operating near 0.351 μm. This cw beam is inserted into the infrared pulsed beamline through a dichroic beamsplitter located just ahead of the frequency tripling system. The collimation of the cw laser and the pulsed beam are initially adjusted to the same value by means of shearing interferometry. A series of shots on flat foil targets is then taken at focus lens positions relative to the target plane during which x-ray pinhole photographs of the target emission are taken. The plane of best focus is then determined from the x-ray pinhole photographs. Due to the presence of residual spherical aberration on the cw UV alignment beam, we select the annular zone on the focusing lens which produces the best focus condition for the cw beam using a Foucault, or knife-edge test in the target plane. Once this reference is established, the plane of best focus may be reliably located over a period of up to several months using only the cw beam.

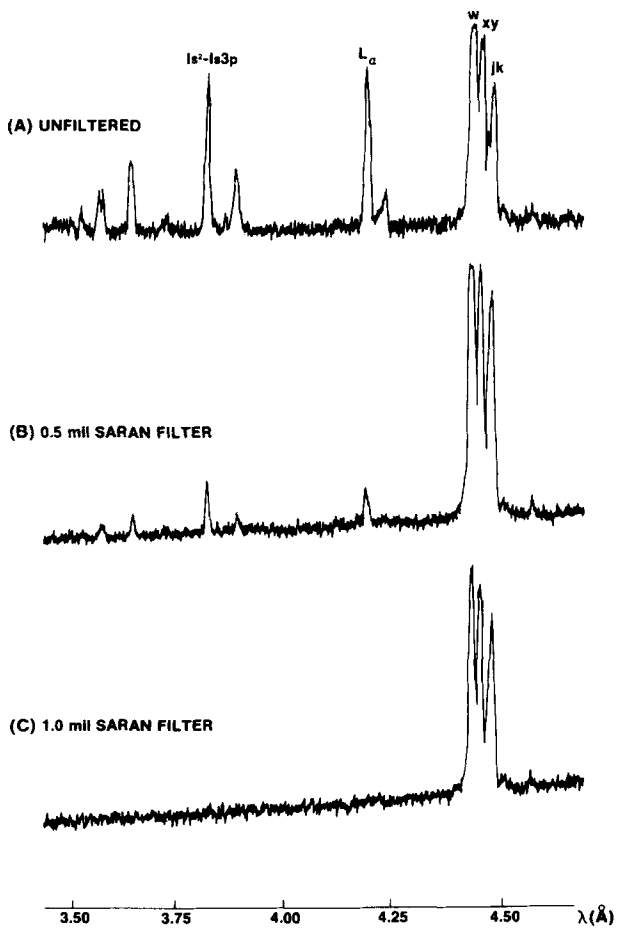

FIG. 2. Monochromatization of laser plasma x-ray line emission by means of foil filtration.

The laser energy which can be delivered to targets at 0.351 μm is presently limited by damage to the dielectric coatings on the laser beam transport optics, which occurs at intensities lower than that for corresponding infrared coatings.[13] Maximum pulse energies of 50–60 J in a 12.5-cm-diam beam have been safely produced. In the plane of best focus this corresponds to an intensity of approximately 10^{15} W/cm^2.

Figure 2 illustrates typical features of the x-ray emission spectrum obtained under these conditions from foil targets. Figure 2(a) shows a microdensitometer scan of the soft x-ray emission recorded on a slitless, flat crystal spectrograph from a target made from commercial Saran ($C_2H_2Cl_2$). The principal emission lines arise from single electron transitions to the ground state in helium-like and hydrogen-like chlorine (atomic number, $Z = 17$). A few of the lines arise from transitions from doubly excited levels in helium-like and lithium-like chlorine. For elements with $Z \geqslant 16$, the k-absorption edge of the neutral material is located very slightly higher in energy than the ls^2–$ls2p$ transition and its associated satellite lines. Hence, a foil of the neutral emitting ion may be used to monochomatize the x-ray source. Figures 2(b) and 2(c) show spectra recorded from Saran targets with 12.5- and 25-μm Saran foils, respectively, placed in front of the spectrograph. The 25-μm foil transmits 50% of the resonance line radiation shown while effectively suppressing all other lines. These spectra are displayed with relatively high dispersion; the overall bandwidth of the transmitted lines in Fig. 2(c) is 8×10^{-3}, which is quite satisfactory for low angle diffraction experiments.

II. X-RAY OPTICS

Since the x-ray emission from these targets is roughly isotropic, the design of high-intensity x-ray beamline facility presents a challenge in maximizing the collection and transport of x rays. Furthermore, in an application such as low angle diffraction, the residual divergence of the beam limits

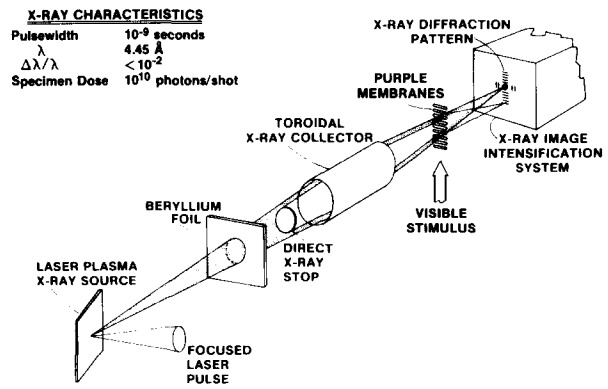

FIG. 3. Conceptual layout of pulsed x-ray diffraction experiment.

the angular resolution of the system. This constrains the x-ray collection system to be a focusing system. The point nature of the laser-driven source, combined with its highly reproducible position in space, is very important because it permits use of a simple, high efficiency, grazing angle focusing system.

Our design is shown schematically in Fig. 3. We use a toroidal mirror in the form of a truncated ellipsoid to focus the x rays. Toroidal x-ray collectors pioneered by Henke[14] and Elliot[15] have collection efficiencies up to a factor of 100 times those of traditional, Franks, bent mirror optics. Our mirror was fabricated from a CERVIT™ substrate in the optical shop at the University of Rochester and coated with nickel in the LLE target fabrication facility. The mirror surface has an inside diameter of 2 cm and an overall length of 9 cm. The radius of the inside surface in the meridian plane is approximately 65 m and has a focal length of 86 cm. In this geometry, it can be shown that the maximum useful collection solid angle is of the order of θ_c^2, where θ_c is the critical angle for total reflection of x rays.[14] The critical angle depends upon the material properties of the mirror surface as well as the x-ray wavelength. Nickel is a good x-ray reflector in the 2- to 5-Å range and results in a collection solid angle for our system of approximately 2×10^{-4} sr. The specular beam reflected from this mirror has an annular structure which must be taken into account in preparing and aligning specimens in the camera.

A space of approximately 20 cm in front of the x-ray detector and camera focus is available to position specimens. The space is isolated from the rest of the laser-plasma target chamber by a vacuum window, allowing the specimen environment (temperature, atmosphere, humidity, etc.) to be controlled by the experimenter. On the vacuum side of the window, a narrow annular stop absorbs most of the nonspecular x rays scattered from the finite microstructure of the mirror surface.

Although it can produce good focusing of radiation from a point source, this single element, ellipsoidal mirror is not an imaging system, as it exhibits severe coma for off-axis points. To obtain good performance, it is, therefore, necessary to carefully align this component. We carry out the alignment using the following procedure. A 633-nm He–Ne laser beam is directed through our vacuum chamber to serve as an initial alignment reference for the laser target, x-ray mirror, and camera detector. In our facility the x-ray camera is mounted with its axis at 45° to the pulsed laser focusing axis in the horizontal plane. With all components approximately positioned, the He–Ne beam is expanded by a 10× microscope objective and focused approximately at the UV laser focus by a $f/2.8$ photographic lens (Bausch and Lomb Super Baltar). The x-ray focusing mirror is then positioned to focus the diverging optical beam from the He–Ne onto the detection plane of the camera. Longitudinal focusing is accomplished by means of a knife-edge test in the detector plane. Lateral alignment is performed by projecting the focal spot with another microscope objective and adjusting for the highest symmetry in the shape and illumination of the numerous diffraction rings produced by the annular nature of the toroid. Several iterations of lateral translations and tilts may be needed to adjust to a predetermined focal point. Once these adjustments are completed, it is then necessary to ensure that the laser plasma is formed precisely at the prime focus of the He–Ne system on each shot. We accomplish this by placing a thin aluminum foil on the laser target holder and positioning this foil at the He-Ne focus by using the edge of the foil as a knife edge (although the plane of this foil is at 45° to the He–Ne axis it causes no difficulty in this adjustment). The pulsed laser is then fired at low energy, typically 100 mJ at 0.351 μm, in order to drill a small pinhole in the aluminum foil. The cw argon-ion laser is then inserted into the pulsed laser beamline and a beamline mirror is adjusted until the focus of this beam passes cleanly through the pinhole. The pinhole is then translated until it passes the He–Ne focus. The final mirror in the pulsed laser beamline is then adjusted to bring the argon-ion laser beam through the pinhole once again. This ensures that the pulsed and cw UV beams and the He–Ne beam and, hence, the x-ray camera source position are coincident in space to within $\pm 20\,\mu$m.

Once an initial alignment of the x-ray camera has been carried out, the pinhole drilling and UV laser alignment procedure requires approximately 10 min to complete. We find it necessary to carry out this procedure only once a day, while the day-to-day drift in this adjustment is of the order of 100 μm or less. This adjustment is performed at the beginning of each dedicated shot day.

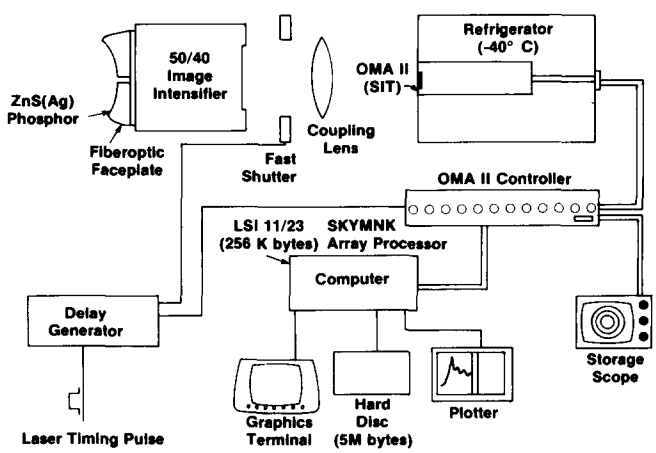

FIG. 4. Two-dimensional video digital image acquisition system.

III. DETECTOR

A schematic diagram of our detection system is shown in Fig. 4. In test shots described below, up to 10^{10} photons of foil-filtered x rays at 4.45 Å were delivered to specimens on each GDL laser shot. Because of the unprecedented rate of delivery of x rays in this system it is impossible to use counter tubes as detectors. Solid-state detectors have many desirable characteristics, but are not yet available in sufficiently large area arrays to be suitable for our application, while film is not sensitive enough to record good patterns with presently available fluxes. On the other hand, TV detectors have no soft x-ray response because of the windows used. This latter problem may be overcome by using a thin scintillator material to convert the x rays to visible light.[16]

In order to efficiently utilize a scintillator detector, we had to overcome a problem posed by the use of high numerical aperture, toroidal focusing optics in an x-ray diffraction camera: the true focal surface of the camera is a sphere tangent to the focal point of the camera and to the vertex of the specimen.[14] The effects of this curvature are not noticed in long focal length or low numerical aperture systems because they exhibit a large depth of focus. However, our early experiments with flat scintillator plates limited our observation to low scattering angles due to limited focal depth. Our goal was to achieve satisfactory focus at up to 35° scattering angles over a 40-mm-diam detection field, which requires a specimen position as close as 3.5 cm from focus. We estimated that a section of a spherical focal surface 5 cm in diameter would permit such a close working distance to be achieved with acceptable sharpness. Satisfactory deposition of a thin ZnS:AG scintillator onto a glass surface of this curvature was achieved by Thomas Electronics, Inc. when the plates were supplied with a 3.2-mm hole drilled at the vertex. This hole also served the zero order (direct) beam stop.

The output of the scintillator is fiber-optically coupled to a VARO 50/40 mm microchannel plate (MCP) image intensifier set to a gain of 30 000. This coupling is facilitated by having the scintillator deposited on a curved surface formed directly on a solid fiber-optic plate. In our present camera, we use a special plate in which the individual fiber axes are at near-normal incidence to both the curved scintillator surface as well as to the flat output surface. Although such a design introduces distortion into the two-dimensional field, it has exhibited the most uniform sensitivity of any configuration we have tried. It was necessary to adopt this geometry because scintillator emission will not couple into fibers which have ends cut at a steep angle to the fiber axis.

The MCP intensifier output is imaged using a Wollensack $f/1.9$ oscillograph lens onto the input of a Princeton Applied Research (PAR) 1254 Silicon Intensified Target (SIT) TV detector. The input to the lens is shuttered by Ilex #4 42.5-mm electrically driven shutter. The SIT is kept at -25 °C in a PAR 1213 refrigeration unit to reduce dark current during an image acquisition sequence and slow-scan readout.

Scan instructions are issued to the SIT tube by a PAR 1216 controller. The 1216 also acquires and digitizes the output of each pixel of the 1254 via a 14-bit A/D. The 1216 controller allows up to 255 TV lines to be scanned with up to 512 channels per line. Channel readout time may be adjusted from 20 to 140 μs. Our readout format includes 224 lines of 448 channels per line. Channel dwell time is typically 140 μs; thus, an entire scan requires 14 s. The target is scanned three consecutive times to fully readout a pattern. The readout electron beam is set to 7.5 V compared to 5.0 V during target preparation. High-voltage multiple scan readout provides more complete image readout with increased dynamic range.[17,18]

The 1216 controller is interfaced to an LSI 11/23 [Digital Equipment Corporation (DEC)] via a DRV-11 parallel interface card. The 11/23 has been modified to accommodate 1 Mbyte of main memory addressed through memory management. The 11/23 sends scan parameters to the 1216, as well as acquiring and summing digitized images into memory. Raw data images are temporarily stored on a DEC RL-01 hard disk system with 5 Mbyte capacity, before archival storage on magnetic tape.

All programming is performed in the computer language FORTH. FORTH is a programming system which was originally developed for telescope control and image processing over 10 years ago.[19] Since then it has been found useful for a variety of process control and data-acquisition applications ranging from satellite control and laser fusion diagnostics to video arcade games. FORTH is a combination of an operating system, a high-level programming language, an assembler, compiler, and an interpreter.[20] It operates as a virtual machine, like a reduced instruction set computer, running on a host computer. Host computers include most microprocessors and minicomputers. It allows an efficient, and modular form of programming by composing functions, or words, out of existing functions. These words can be treated either as programs (and run directly from the keyboard or from disk), or as subroutines and embedded within other words. With the assembler, codes can quickly be optimized in-line.

FORTH systems are constructed of either direct or indirect threaded code, hence, can fit within 16 kbytes and may include memory management, multitasking, and multiprogramming capabilities. Their run time speed is about ten times faster than BASIC, and, depending upon the application, may be 1/2 that of FORTRAN or ASSEMBLY language. The FORTH assembler essentially allows creation of codes to run at the machine speed of the PDP 11/23. The simplicity of the FORTH system allows very easy access to, and efficient use of, computer hardware and peripherals.

For computationally intensive applications, such as diffraction image processing, high-level FORTH is inefficient. Thus, for analysis we use mostly FORTH assembly language with floating point computations performed on the SKYMNK-02 array processor (Sky Computer). We have choosen to run the SKYMNK-02 under FORTH rather than FORTRAN to provide a compact and unified data-acquisition and computation facility.

Our FORTH SKYMNK driver includes a SKYMNK command block construction and execution routine, one- and two-dimensional FFT routines, as well as debugging aids. SKYMNK blocks may be constructed just prior to execution. However, for programs requiring extreme speed of

execution we have developed a command block compiler (CBC). The CBC compiles into command block lists, programs of arbitrary command block length. Each block in a list is headed by a data word containing the word length of the block (one, three, seven, or ten words). Each program is headed by 2 bytes containing the number of blocks in the program. The compiled programs are identified by their stored memory location. During execution the program identifies the number of blocks in the program, strips off the block length headers, and sequentially ships command blocks to the SKYMNK. After shipping each block the supervisory program checks the SKYMNK command queue to make sure the 13 block command queue depth is not exceeded.

Depending on the task, and the amount of control structure required between complied groups of SKYMNK blocks, this software runs 10 to 20 times faster than equivalent PDP 11/23 machine code. Our application programs include vectorized square-root computations, image geometric distortion and intensity correction routines as well as intramemory image moves and Fourier analysis.

IV. SPECIMEN CHAMBER

The end plate of the camera, which supports the scintillator/MCP assembly, is attached to a 10-in.-diam by 10-in.-long chamber constructed from two tubular subassemblies. Each subassembly has four portholes arranged at 90°. One subassembly has 2-in.-diam ports while the other has 4-in.-diam ports. These subassembles may be installed in either sequence, allowing maximum flexibility in the use of the ports to support micromanipulators, windows, beam splitters, gas, water, and electrical feedthroughs, etc. The specimen chamber may be exposed directly to the laser target chamber vacuum, and may be isolated from vacuum by transparent and/or light-tight vacuum windows. Specimen cassettes may be installed with controlled or sealed atmospheres, and cassette temperatures may be regulated by a water bath.

Specimen cassettes are conveniently aligned by means of the He–Ne alignment laser beam, and can readily be replaced between laser shots at the 30-min shot interval when using the transparent vacuum window. A magnetic, snap-on, light-tight beryllium window 1 mil thick prevents specimen exposure to scattered laser light through the transparent window on a target shot. Because many experiments involve delivering a controlled flash of light to the specimen prior to x-ray diagnosis, the scintillator plate is also covered with a 1-mil-thick, light-tight beryllium window.

V. EXPERIMENTAL RESULTS

We now present some x-ray diffraction patterns from biological specimens to illustrate the performance capabilities of the facility. Biological specimens present especially challenging tests because of their relatively low x-ray scattering power. The operation of the facility for kinetic experiments will be described; however, detailed results on photostimulated membrane systems will be presented elsewhere.[21] The results were all obtained using foil-filtered soft x-ray radiation at 4.45 Å produced from laser irradiated Saran targets. This wavelength was chosen to enable very thin specimens to be used while maintaining good x-ray scattering efficiency. Our interest in thin specimens was derived from our desire to perform photostimulation on optically dense specimens.

A photobiological system of widespread interest in recent years is the purple membrane (PM) of the *Halobacterium halobium*. This membrane is composed of an almost perfect, hexagonally packed, two-dimensional array of one protein, bacteriorhodopsin (BR).[22] Like mammalian rhodopsin, BR contains the chromophore retinal and has a photocyle with a time course and spectral characteristics similar to rhodopsin.[23] It has been shown that BR functions as a light-driven proton pump which sets up a transmembrane hydrogen-ion gradient.[24] It is of interest to determine if molecular conformational changes are associated with the ion pumping function. The PM serves not only as a demonstration system for low angle x-ray diffraction, but may be used to demonstrate some of the techniques which must be employed in kinetic experiments.

Figure 5 shows a powder diffraction pattern from a dried pellet of purple membrane recorded by using a single, nanosecond duration, laser pulse of 45 J at 0.351 μm. The diffraction pattern consisted of a set of bright circular rings on the scintillator detector, a sector of which was circularly averaged by the 11/23 computer to produce this display. The specimen consisted of an array of membrane fragments or platelets, whose planes were partially oriented by drying onto a (1–2 μm) polypropylene support. The highest-order reflection shown corresponds to 7-Å resolution in the plane of the membrane (and is the highest-order reflection to be reliably phased by any group to date). The reflections are all indexed on a hexagonally packed lattice after Blaurock and Stoeckenius.[22]

Because of our interest in the photokinetic structural behavior of purple membrane, the x-ray diffraction camera was configured to support the requirements for such experiments. These requirements included the need for maintaining a controlled environment for the specimen while trans-

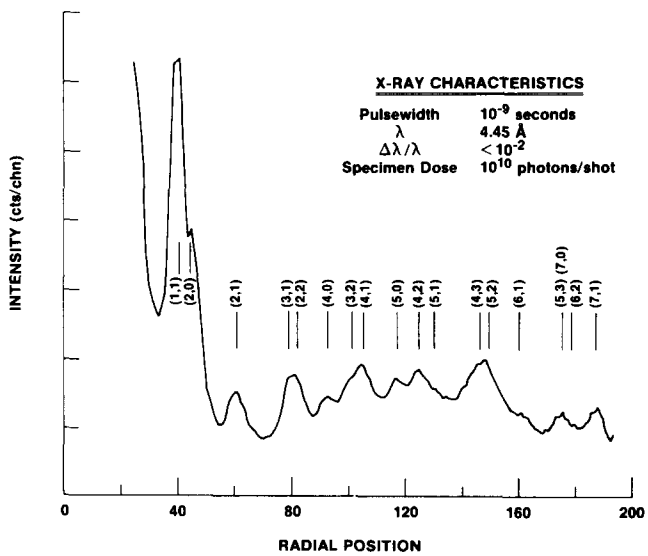

FIG. 5. Circular average of purple membrane diffraction.

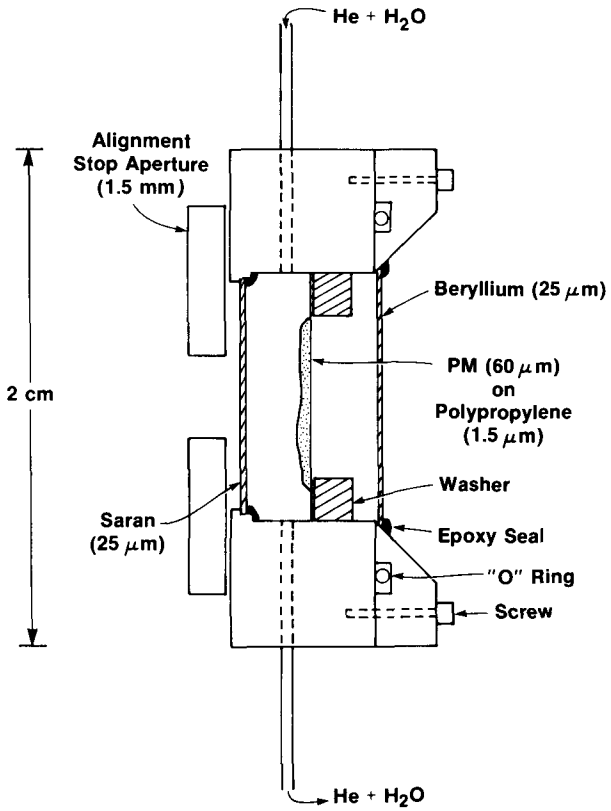

FIG. 6. Sample chamber.

porting synchronized optical and x-ray pulses to the specimen. A thin specimen chamber, shown in Fig. 6, was constructed which permits a supply of gas to flow across the specimen and which has an entrance window transparent to both light and x rays. When using 4.45-Å radiation a Saran window may be used. (Commercial Saran will withstand a pressure differential of up to 1 atm over apertures as large as 1 cm^2, permitting evacuation of the surrounding chamber, if desired. However, we have often taken data with the surrounding chamber filled with 1 atm of dry helium with no loss in performance.) The exit window material has been either Saran, thin polypropylene, or beryllium. When Saran is used, we maintain the overall thickness of this material in the x-ray path of 25 μm for optimal spectral filtration and transmittance.

Optical stimulation pulses are delivered through the specimen holder entrance window using the arrangement shown in Fig. 7. A dichroic beam splitter consisting of a 1.5-

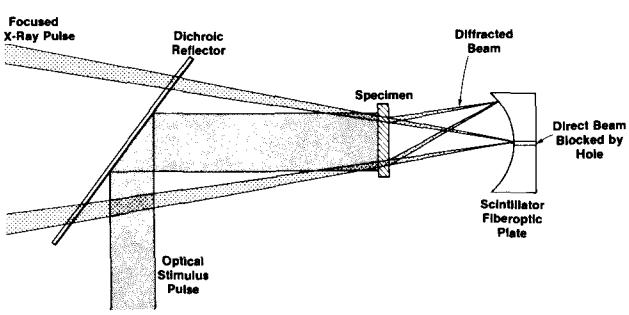

FIG. 7. Arrangement for photoinduced structural kinetic experiments.

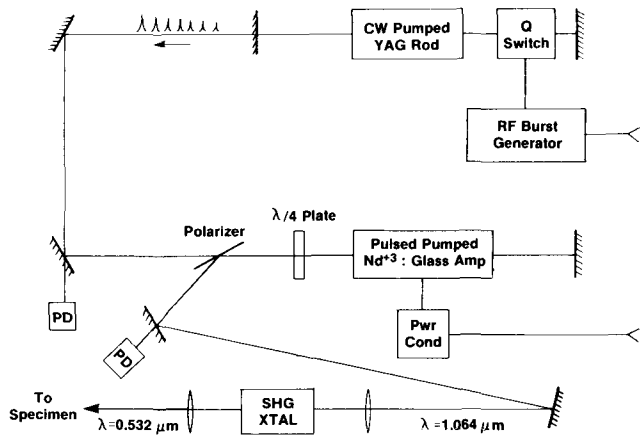

FIG. 8. Photostimulus system for purple membrane.

μm-thick Mylar foil coated with approximately 2000 Å of aluminum, fabricated by Merle Hirsch Associates, is used to direct light pulses along the axis of the x-ray camera.

In the design of a kinetic x-ray diffraction experiment, it must be kept in mind that diffraction is a technique which probes the average structure of bulk material. If a structural perturbation is to be introduced, care must be taken to uniformly perturb as high a fraction of the specimen as possible to minimize the ambiguity inherent in interpreting data acquired from a mixed phase system. Purple membrane is typical of many photoactivated systems which might be studied in that it exhibits a finite quantum efficiency for photoactivation, in this case, 30%.[25,26] Because we were interested in the study of structural activity during the formation of a stable photointermediate state of the system, we decided to employ a train of light pulses to successively raise an increasing fraction of the system to the photoactive state. This strategy was dictated by the fact that prior to the formation of a stable photointermediate, the presence of light maintains an equilibrium between the ground state and photocycling populations. Although the details of this strategy are specific to the system under study, the operation of our stimulus system illustrates the general features of any such experimental system.

Our photostimulation system is shown in Fig. 8. A cw-pumped, acousto-optically Q-switched, Nd^{+3}:YAG laser (Control Laser Model 510) is used to generate a pulse train at a wavelength of 1.064 μm. The Q switch is driven by a radio-frequency burst generator which allows control of the overall length of the pulse train. Typically, we produce a train of six, 150-ns-wide, laser pulses separated by approximately 45 μs. The rf burst generator is triggered by a digitally delayed clock pulse from the computer which fires the GDL system, thus allowing synchronization of the optical and x-ray pulses. The pulse train is amplified by a 12-mm-diam Nd^{+3}:glass rod used in a double pass configuration. The amplifier is triggered by a digital delay channel parallel to the Q-switch driver channel. The amplified train is then frequency doubled by a temperature-tuned CDA crystal (Quantum Technology) with an overall conversion efficiency of approximately 10%. The frequency doubled light pulses are transmitted to the x-ray camera using four dielectric coated mir-

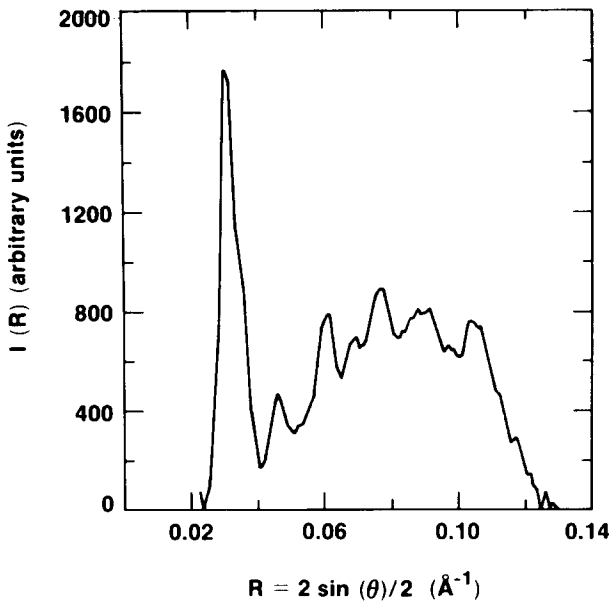

FIG. 9. Circular average of photostimulated PM.

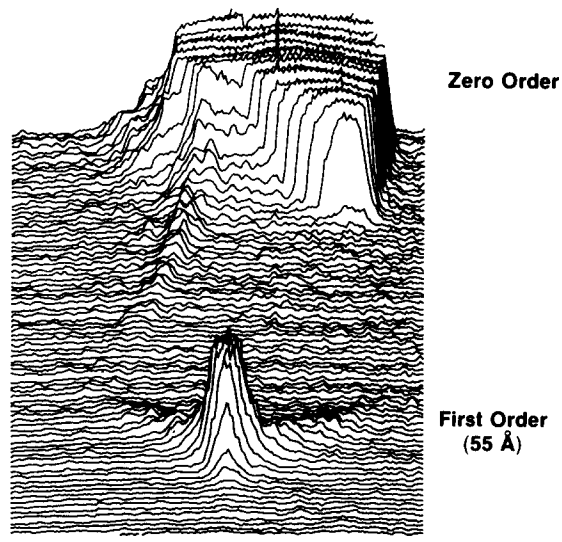

FIG. 10. Dipalmitoyl lecithin x-ray diffraction.

rors which reduce the energy content of the beam at the fundamental wavelength to less than 10% of the second-harmonic energy.

An x-ray diffraction pattern from purple membrane recorded approximately 1 ns after photostimualation by the above system is shown in Fig. 9. Several significant changes to the intensities of many of the reflections are observed. For example, there is a reversal in the intensity between the (3,2) and (4,1) reflections and the decrease in the (5,0) relative to the (4,2) reflection. A detailed discussion of a series of such measurements will be given elsewhere, but it is clear that significant structural activity is present on this time scale.

The above stimulation system allows us to explore such changes with a controlled delay down to a few microseconds, which is the jitter time in the appearance of the pulse from the present GDL oscillation system. To perform optical stimulation experiments at shorter delay time, a harmonic component derived from the GDL system itself would be used, yielding an ultimate time resolution of the order of the 1-ns x-ray pulse itself.

The lattice constant in purple membrane is approximately 63 Å and much of the structural activity is observed at substantially smaller scale length. In other membrane systems and in many polymer studies, however, much longer scale lengths are of interest. Thus the low angle performance of the camera system is important. In Fig. 10, we present a portion of a digital image showing the first order lamellar diffraction from a dipalmitoyl lecithin multilayer structure with a basic repeat period of 55 Å. This specimen was placed approximately 20 cm from the focus of the camera, and foil filtered x-ray radiation at 4.45 Å was used. The specimen was oriented in a low angle, reflection geometry and intercepted only a small portion of the annular, x-ray beam. The natural mosaic structure of the multilayer is evident in the pronounced, arc-like scattering around the (saturated) central reflection peak. The large space between this peak and the zero order suggested that a much lower angle reflection could be observed. These results suggest many possible studies of dynamic structural phenomena in materials with large repeat distances.

ACKNOWLEDGMENTS

We are grateful to Dr. J. Lanyi for the PM preparations, to F. Kirkpatrick, B. Fung, and M. Nicholson for facilities for washing the PM, to J. Abate, B. Flaherty, W. Lockman, and T. Kessler for operating the laser, L. Forsley for assistance in computer programming, J. Chao for help with interfacing the OMA and LSI11/23, and H. Graf for fabrication of the toroidal x-ray collector. This work was supported, in part, by the National Science Foundation, Grant No. PCM 79-04375, and by the National Institute of Health, Grant No. 1R01 GM-27354-01. This work was partially supported by the following sponsors: Empire State Electric Energy Research Corporation, Exxon Research and Engineering Company, General Electric Company, New York State Energy Research and Development Authority, Northeast Utilities, The Standard Oil Company (OHIO), and the University of Rochester. Such support does not imply endorsement of the content by any of the above parties.

[1] A. Bienenstock and H. Winick, Phys. Today **36**, 48 (1983).
[2] *Physics Today*, May 1981 is a special issue on synchrotron radiation including the following articles: E. M. Rowe, "Facilities in the United States"; C. J. Sparks, Jr., "Research with X-rays"; H. Winick, G. Brown, K. Halbach, and J. Harris, "Wiggler and Undulator Magnets"; D. E. Eastmen and F. J. Himpsel," Ultraviolet Radiation—An Incisive and Versatile Tool."
[3] H. E. Huxley, A. R. Faruqi, J. Bordas, M. H. J. Koch, and J. R. Milch, Nature **284**, 140 (1980).
[4] R. D. Frankel and J. M. Forsyth, Science **104**, 622 (1979).
[5] R. D. Frankel and J. M. Forsyth, in *Methods in Enzymology*, edited by L. Packer (Academic, New York, 1982), Vol. 88, p. 276.
[6] B. Yaakobi, P. Bourke, Y. Conutrie, J. Delettrez, J. M. Forsyth, R. D. Frankel, L. M. Goldman, R. L. McCrory, W. Seka, and J. M. Soures, Opt. Commun. **38**, 196 (1981).
[7] W. Seka, J. M. Soures, O. Lewis, J. Bunkenburg, D. Brown, S. Jacobs, G. Mourou, and J. Zimmerman, Appl. Opt. **19**, 409 (1980).
[8] J. F. Hoose, SPIE **103**, 22 (1977).

[9]W. Seka, S. D. Jacobs, J. E. Rizzo, R. Boni, and R. S. Craxton, Opt. Commun. **34**, 469 (1980).
[10]W. Seka, J. M. Soures, S. D. Jacobs, L. Lund, and R. S. Craxton, IEEE J. Quantum Electron. **QE-17**, 1689 (1981).
[11]B. Yaakobi, T. Boehly, P. Bourke, Y. Conturie, R. S. Craxton, J. Delettrez, J. M. Forsyth, R. D. Frankel, L. M. Goldman, R. L. McCrory, M. C. Richardson, W. Seka, D. Shvarts, and J. M. Soures, Opt. Commun. **39**, 175 (1981).
[12]W. Seka, R. S. Craxton, J. Delettrez, L. M. Goldman, R. Keck, R. L. McCrory, D. Shvarts, J. M. Soures, and R. Boni, Opt. Commun. **40**, 437 (1982).
[13]J. A. Abate, R. Roides, S. D. Jacobs, W. Piskorowski, and T. Chipp, in *Proceedings of the 14th Annual Symposium on Optical Materials for High Power Lasers*, edited by A. H. Guenther, H. E. Bennett, B. Newman, and D. Milam, NBS Special Publication 669 (National Bureau of Standards, U. S. GPO, Washington, D.C., 1984).
[14]B. L. Henke and J. W. M. DuMond, J. Appl. Phys. **26**, 903 (1955).
[15]A. Elliott, J. Sci. Instrum. **42**, 312 (1965).
[16]G. T. Reynolds, J. R. Milch, and S. M. Gruner, IEEE Trans. Nucl. Sci. **NS-24**, 501 (1977).
[17]H. Staerk, R. Mitzkus, and H. Meyer, Appl. Opt. **20**, 471 (1981).
[18]G. W. Liesegang and P. D. Smith, Appl. Opt. **20**, 2604 (1981).
[19]C. Moore, J. Astron. Astrophys. Suppl. **15**, 497 (1974).
[20]P. M. Kogge, IEEE Trans. Comput. **15**, 22 (1982).
[21]R. D. Frankel and J. M. Forsyth, Biophys. J. (to be published).
[22]A. E. Blaurock and W. Stoeckenius, Nature New Biol. **233**, 153 (1971).
[23]M. Ottolenghi, in *Methods in Enzymology*, edited by L. Packer (Academic, New York, 1982), Vol. 88, p. 470.
[24]D. Oesterhelt and W. Stoeckenius, Proc. Natl. Acad. Sci. USA **20**, 2835 (1973).
[25]C. R. Goldschmidt, O. Kalisky, T. Rosenfeld, and T. M. Ottolenghi, Biophys. J. **17**, 179 (1977).
[26]O. Kalisky, C. R. Goldschmidt, and M. Ottolenghi, Biophys. J. **19**, 185 (1977).